GeoVadis: The Future of Geotechnical Engineering – Juneja, Joseph & Dasaka (Eds)

Analytical estimation of the dynamic response of ballasted tracks considering subgrade degradation

R.S. Malisetty and B. Indraratna
1Transport Research Centre, University of Technology Sydney, Ultimo, Australia

ABSTRACT: Track layers including ballast and subgrade degrade with repeated train passes, while this degradation can in turn affect the track critical speed as well as the dynamic stresses. This paper discusses a combined rheological-continuum analytical approach to estimate the influence of subgrade degradation on the track response. The track substructure with ballast, capping and subgrade layers are considered as continuum layers allowing the propagation of Rayleigh waves generated by moving trains. Representing mud pumping commonly observed in Australian rail tracks, empirical relationships capturing progressive degradation of subgrade modulus are adopted and combined with the analytical approach. Results showed that subgrade degradation is affected significantly by the dynamic stresses, while the critical speed is reduced. As the speed and axle load increases, degradation occurs at an increasing rate, propagating to greater depths leading to mud pumping. A new critical number of load cycles is calculated that will provide information on the length of the train for different axle loads and train speeds when travelling on vulnerable subgrades.

1 INTRODUCTION

The 21st century globalization and technological advancements has necessitated faster and efficient transport networks to meet the supply chain requirements all over the world. High speed trains passenger trains with train speeds exceeding 300 km/h use both ballasted and slab tracks which provide distinct advantages in different aspects. On the other hand, freight trains have been carrying heavier loads than before, while also travelling at medium high speeds. In some countries, the maximum axle load of freight trains reaches upto 42 tonnes, while the maximum speed of heavy haul freight trains with train speeds reaching 130 km/h.

The adverse effects of increasing speeds on the track vibrational response were studied by several researchers employing different techniques such as 2D and 3D analytical models (Sheng et al. 1999, Mezher et al. 2016, Punetha et al. 2020) Finite Element (FE) models (Bian et al. 2016, Sayeed & Shahin 2016, Tucho et al. 2022) and field studies (Kaynia et al. 2000, PRIEST et al. 2010, Connolly et al. 2014). These studies highlighted that displacements, peak particle velocities and accelerations within track substructure as well as near-field become amplified with increasing train speeds. This amplification occurs due to resonance between train speed and the characteristic surface wave speed of the track substructure. The train speed at which the peak response is achieved is considered as the 'critical speed' of the track, which is predominantly dependent on the shear modulus of softest track layer usually subgrade (Suiker et al. 1999).

A few studies (Yang et al. 2009, Tucho et al. 2022) highlighted the amplification of stress response within the track layers, where increasing train speed not only caused increase in vertical stress, but also led to greater effects of principal stress rotation. While past researchers only focused on the transient response of track, it is important to consider the effect of these amplified stresses on the permanent response of track materials. This is especially important for optimizing maintenance of ballasted tracks in heavy haul railway networks as heavier loads often cause track degradation such as ballast breakage, differential settlements,

DOI: 10.1201/9781003645931-98

subgrade pumping and the associated fouling of ballast layer (Indraratna et al. 2022, Malisetty et al. 2020, Nimbalkar & Indraratna 2016). In this context, this paper presents an analytical methodology to simulate the influence of increasing train speeds and heavy axle loads on the degradation response of soft subgrades under vulnerable conditions. Based on the model predictions, critical number of loading cycles is proposed which provides the number of passes of a freight train on a track with softer subgrade.

2 METHODOLOGY

The ballasted railway track is modelled using a 2D analytical framework proposed by Malisetty & Indraratna (2024) as shown in Figure 1. A n-layer track substructure is considered which consists of ballast, capping and other substructure layers which is modelled using a 2D continuum in the x-z plane, where x denotes the direction of train movement, while z denotes the depth of the track. By considering the substructure as a 2D continuum, the model benefits from simulating the plane body wave propagation in the x-z directions, thus able to predict the dynamic response in track layers. Within the 2D continuum, the Cauchy stress vectors (σ'_{ij}) in the x-z direction in the n^{th} layer can be written as:

$$\sigma'^{\,n}_{ij} = \lambda^n \delta_{ij} \varepsilon^n_{kk} + 2\mu^n \varepsilon^n_{ij} \tag{1}$$

where, λ and μ are the Lames constants which are functions of elastic modulus (E), Poisson's ratio (v) and density (ρ) of the layer. ε_{ij} is the strain tensor, while $\varepsilon^n_{kk} = \varepsilon^n_{xx} + \varepsilon^n_{zz}$ is the volumetric strain in the x-z direction.

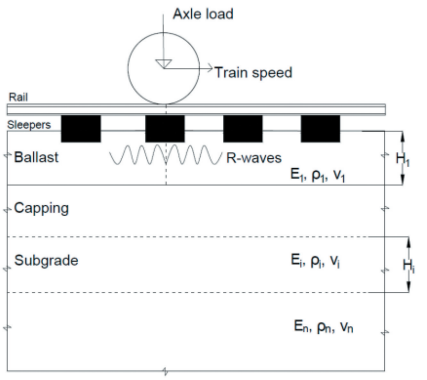

Figure 1. Substructure model considered in this study.

Considering Rayleigh wave propagation in the track layers, the strains can be expressed in terms of displacements given as:

$$\varepsilon_{ij} = \begin{bmatrix} \frac{\partial u_x}{\partial x} & \frac{1}{2}\left(\frac{\partial u_x}{\partial y} + \frac{\partial u_y}{\partial x}\right) \\ \frac{1}{2}\left(\frac{\partial u_x}{\partial y} + \frac{\partial u_y}{\partial x}\right) & \frac{\partial u_z}{\partial z} \end{bmatrix} \tag{2}$$

where, $u_x = \frac{\partial \emptyset}{\partial x} - \frac{\partial \varphi_y}{\partial z}$, $u_z = \frac{\partial \emptyset}{\partial z} + \frac{\partial \varphi_y}{\partial x}$

The compression wave potential ($\emptyset_n$) and shear wave potential (Ψ_{y_n}) can be written as harmonic wave forms given as:

$$\emptyset_n = \exp(i(\omega t - kx)).\left\{A_{pn1}\exp\left(i\xi_{pn1}z\right) + A_{pn2}\exp\left(i\xi_{pn2}z\right)\right\} \tag{3}$$

$$\Psi_{y_n} = \exp(i(\omega t - kx)).\{A_{sn1}\exp(i\xi_{sn1}z) + A_{sn2}\exp(i\xi_{sn2}z)\} \tag{4}$$

$$\xi_{pn1,2} = \pm\sqrt{\frac{\omega^2}{C_p^2} - k^2} \quad ; \quad \xi_{sn1,2} = \pm\sqrt{\frac{\omega^2}{C_s^2} - k^2} \tag{5}$$

$A_{pn1,2}$ and $A_{sn1,2}$ are the amplitudes of wave potentials, while ω and k are the angular frequency and wave number of the R-waves, C_P and C_s are the velocities of compression and shear waves in the n^{th} layer. For simulating R-wave propagation and estimating the stresses in the shallow track layers, stress and displacement compatibility boundary conditions are applied at the top surface and layer interfaces. For this study, three-layer continuum is considered with ballast of thickness H_1, capping of thickness H_2 and subgrade (halfspace) layers, which will result in 10 boundary conditions as follows:

At top surface i.e., Z=0, $\sigma_{zz}^{'1} = P_{SB}$; $\sigma_{zx}^{'1} = 0$

At ballast capping interface i.e., Z= H_1, $\sigma_{zz}^{'1} = \sigma_{zz}^{'2}$; $\sigma_{zx}^{'1} = \sigma_{zx}^{'2}$; $u_z^1 = u_z^2$; $u_x^1 = u_x^2$

At capping-subgrade interface i.e., $Z = H_2$, $\sigma_{zz}^{'2} = \sigma_{zz}^{'3}$; $\sigma_{zx}^{'2} = \sigma_{zx}^{'3}$; $u_z^2 = u_z^3$; $u_x^2 = u_x^3$

Substituting stresses from Eq. 1 in the above boundary conditions result in 10 equations that can be written in the matrix form as $A.\ C = P$, where A represents the amplitude matrix, C represents the 10x10 coefficient matrix where all elements are functions of layer properties, ω, k and thickness of layers. P_{SB} represents the stress transmitted to the sleeper-ballast interface by the superstructure system (rails, railpads and sleepers) when a train passes over the rails. A simplified approach is used in this study to calculate the sleeper-ballast interface stress which is given as:

$$P_{SB} = \theta.P_r\left(\frac{1}{2}\cos(\omega_l t) + \frac{1}{2}\right) \tag{6}$$

θ is the superstructure amplification factor which is equivalent to $\sqrt{\frac{K_p^2+\left(C_p\omega_a\right)^2}{\left(K_p-(M_r+M_s)\omega_a^2\right)^2+\left(C_p\omega_a\right)^2}}$, $\omega_l = \frac{3\pi}{2}\left(\frac{K_p}{4EI}\right)^{-1/4}$, where P_r is railseat load, K_p, C_p are the stiffness and damping coefficients of railpads, M_s *and* M_r are the mass of sleeper and rail, respectively, while E and I are the Young's modulus and second moment of inertia of rails. ω_a is the axle loading frequency which is dependent on the train speed (V) which can be written as $\omega_a = 2\pi\frac{V\left(\frac{m}{s}\right)}{axle-axle\ distance}$.

Table 1. Material properties.

Layer	Ballast	Capping	Subgrade	Superstructure
Properties	E = 150 MPa v = 0.35 ρ = 1660 kg/m^3 H = 300mm	E = 180 MPa v = 0.3 ρ = 1900 kg/m^3 H = 200mm	E = 30 MPa v = 0.4 ρ = 1710 kg/m^3 Halfspace	EI = 63e^5 Pa.m^{-4} M_s = 490 kg M_r = 60 kg K_p = 350 MN/m C_p = 1.8e^5 N/m.s

3 RESULTS AND DISCUSSION

The analytical framework is used to predict dynamic stresses in the track substructure layers. For this purpose, typical ballasted railway tracks on the eastern coast of Australia are considered, where the properties of different layers are shown in Table 1. Medium-stiff subgrade conditions are considered, while the ballast and capping layers are considered as per Australian Standards which are obtained from field investigations from (Malisetty & Indraratna 2024, Nimbalkar & Indraratna 2016). Two different cases are considered where case-1 investigates the track with ballast layer laid directly over subgrade, while case-2 involves track with capping as intermediate layer between ballast and subgrade.

Figure 2a shows the model predictions of vertical stresses at 150mm below sleeper soffit for substructure conditions in Case-1. Four axle loads are considered in this study: 20t, 25t, 30t, 35t typically representing freight trains in Australia. As observed from the figure, the vertical stresses increase with increasing train speed and reaches a peak value at a train speed of about 380 km/h. It is to be noted that the increasing the axle load magnifies the vertical stresses but does not affect the critical speed of the track. Figure 2b shows the variation in critical speed of the track, when the subgrade modulus is varied using constant ballast properties. It can be seen that the critical speed follows almost a linearly reducing relationship with drop in E_s of subgrade, where the reduction rate increases when the subgrade becomes really soft with $E_s < 10\ MPa$.

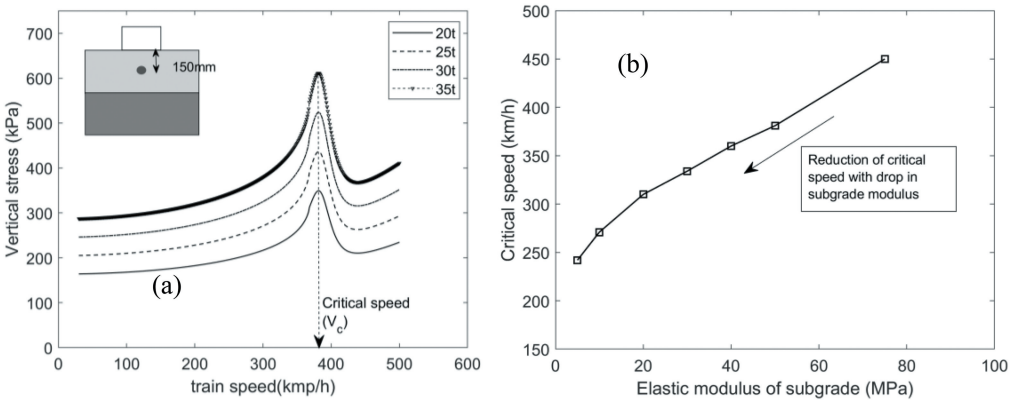

Figure 2. (a) Vertical stress variation with train speeds (b) Variation of critical speed with subgrade modulus.

Figure 3 shows the stress path at different depths in the track substructure under a moving load, where the influence of rotating principal stress axes is clearly visible in the x-z direction. Also, while the vertical stress attenuates with depth, the shear stress (σ'_{xz}) increases till a depth of 0.15m and then reduces. This change in PSR stress path has significant impact on the octahedral (q_d, deviatoric in 2D) stresses in the track layers which will cause degradation of subgrade and other track layers. It is reported that subgrade soils especially present on the southeastern coast of Australia are prone to mud pumping and modulus degradation under unfavorable drainage conditions (Indraratna et al. 2020). Furthermore, the rate of degradation is found to be dependent on the cyclic stress ratio (CSR= $q_d/2\sigma'_c$) imposed by the moving train on subgrade.

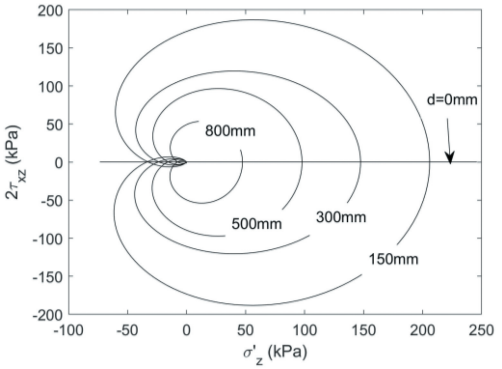

Figure 3. Stress paths with principal stress rotation at different depths in the track (depth from sleeper soffit).

To understand the influence of train speed and the resulting dynamic stresses on subgrade degradation, the empirical equation (Eq. 7) for subgrade degradation (δ_d) proposed by Nguyen et al. (2021) is adopted and implemented in the track model presented earlier. An iterative procedure is adopted where the initial subgrade modulus (G_{s1}) is used to calculate the dynamic deviatoric stress in the subgrade when a train with a particular axle load runs at a certain speed for 1 cycle. After each cycle, the degradation rate is calculated based on CSR and then the track model is updated with the degraded modulus (G_{sN}) in the next cycle. The procedure is continued till the degradation rate reaches 60%, at which failure of samples was observed in laboratory.

$$1 - \delta_d = G_{sN}/G_{s1} = 1 - \log(a.CSR)^b [\log N]^c \quad (7)$$

a, b, c are empirical constants which are taken as 3.34, 0.69 and 2.5, respectively.

Figure 4 shows the rate of degradation of subgrade modulus with number of loading cycles for different axle load trains running at different constant speeds. A reference depth of 0.5m below the subgrade surface is considered for analysing the degradation. When a train with lower axle loads (20t) runs at low speeds (30 km/h), the subgrade degradation reduces and reaches the threshold value at around 3000 loading cycles, which does not pose any risk as it requires higher number of train passes to reach 3000 loading cycles which would give sufficient time for pore water pressures to dissipate. Whereas when the axle load is increased to 30t, the threshold degradation is reached at much lower number of loading cycles (~89). Increasing train speeds with constant axle load is also found to have similar effect where the degradation threshold is reached at 172 cycles for V=130 km/h. The number of loading cycles at which the degradation reaches a threshold is defined as 'critical loading cycles' (N_{crit}). In contrast to the critical speed of the track, the critical number of loading cycles is dependent on the axle load of the train. As can be seen from Figure 4a, N_{crit} not only depends on the operating train speed, but also depends on the axle load of the train. A reference N of 100 is also plotted to indicate the number of load cycles that is equivalent to a freight train with an average length of 100 wagons. It can be observed that if the train speed is increased or if the axle load is increased, the subgrade degrades earlier than the freight train traverses the vulnerable subgrade. This increases the risk of mud pumping, where the subgrade is stable before the train arrival, but the pumping occurs during the passage of a train. For load-speed combination where N_{crit} is higher than 100 cycles, the subgrade degrades but does not reach the threshold value when an average freight train passes, thus increasing the possibility of pore water pressures to dissipate after the train passes. By introducing a capping layer of 200mm thickness, it can be seen from Figure 4a that the degradation rate is slowed down while the critical number of loading cycles increased, thus retarding the subgrade degradation rate.

Figure 4b shows the depth to which the subgrade is prone to mud pumping for different load-speed combinations for both Case-1 and 2. Foe each condition, the depth at which subgrade degradation reaches threshold before 100 cycles is plotted. As observed, the depth of influence increases with increasing train speed or axle load, while the introduction of capping layer reduced the depth significantly for lower axle loads, while higher axle load trains can still cause degradation till very shallow depths within the subgrade (0.1-0.2m).

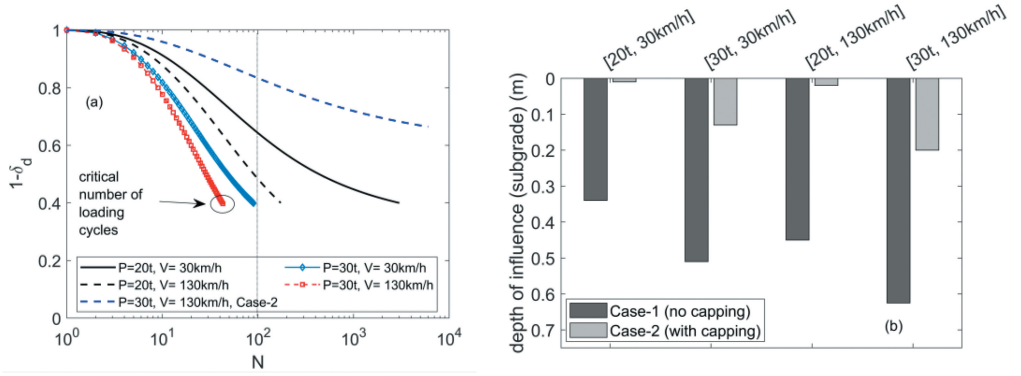

Figure 4. (a) Subgrade modulus degradation with number of loading cycles (b) Maximum depth of influence within subgrade.

4 CONCLUSIONS

An analytical approach is presented in this paper which combines the dynamic amplification of stresses in the track layers at different train speeds with subgrade degradation under vulnerable conditions. It was observed that increasing axle loads as well as increasing train speeds caused dynamic amplification of stresses which led to rapid subgrade degradation causing

mud pumping before a single freight train passes over the vulnerable site completely. Critical number of loading cycles proposed in this study provides information on the potential onset of mud pumping for different train operations. Further, using a compacted capping layer can significantly retard the degradation process, as well as reducing the maximum depth of degradation. The analytical approach is particularly useful for track engineers to gain understanding of the onset of mud pumping and to take decisions on speed and load restrictions on vulnerable subgrades during extreme rainfall events.

ACKNOWLEDGEMENT

This work is funded by Australian Research Council Linkage Project (200200915) and supported by Sydney Trains, Australian Rail Transport Corporation (ARTC), Bentley systems, Bestec instruments and SMEC Australia.

REFERENCES

Bian, X., Cheng, C., Jiang, J., Chen, R. & Chen, Y. 2016. Numerical analysis of soil vibrations due to trains moving at critical speed. *Acta Geotechnica*, 11, 281–294.

Connolly, D. P., Kouroussis, G., Woodward, P. K., Alves Costa, P., Verlinden, O. & Forde, M. C. 2014. Field testing and analysis of high speed rail vibrations. *Soil Dynamics and Earthquake Engineering*, 67, 102–118.

Indraratna, B., Singh, M., Nguyen, T. T., Leroueil, S., Abeywickrama, A., Kelly, R. & Neville, T. 2020. Laboratory study on subgrade fluidization under undrained cyclic triaxial loading. *Canadian Geotechnical Journal*, 57, 1767–1779.

Indraratna, B., Singh, M., Nguyen, T. T., Rujikiatkamjorn, C., Malisetty, R. S., Arivalagan, J. & Nair, L. 2022. Internal Instability and Fluidisation of Subgrade Soil under Cyclic Loading. *Indian Geotechnical Journal*, 52, 1226–1243.

Kaynia, A. M., Madshus, C. & Zackrisson, P. 2000. Ground vibration from high-speed trains: prediction and countermeasure. *Journal of Geotechnical and Geoenvironmental Engineering*, 126, 531–537.

Malisetty, R. S. & Indraratna, B. 2024. Critical speed of ballasted railway tracks: Influence of ballast and subgrade degradation. *Transportation Geotechnics*, 46, 101246.

Malisetty, R. S., Indraratna, B. & Vinod, J. 2020. Behaviour of ballast under principal stress rotation: Multi-laminate approach for moving loads. *Computers and Geotechnics*, 125, 103655.

Mezher, S. B., Connolly, D. P., Woodward, P. K., Laghrouche, O., Pombo, J. & Costa, P. A. 2016. Railway critical velocity – Analytical prediction and analysis. *Transportation Geotechnics*, 6, 84–96.

Nguyen, T. T., Indraratna, B. & Singh, M. 2021. Dynamic parameters of subgrade soils prone to mud pumping considering the influence of kaolin content and the cyclic stress ratio. *Transportation Geotechnics*, 29, 100581.

Nimbalkar, S. & Indraratna, B. 2016. Improved performance of ballasted rail track using geosynthetics and rubber shockmat. *Journal of Geotechnical and Geoenvironmental Engineering*, 142, 04016031.

Priest, J. A., Powrie, W., Yang, L., Grabe, P. J. & Clayton, C. R. I. 2010. Measurements of transient ground movements below a ballasted railway line. *Géotechnique*, 60, 667–677.

Punetha, P., Nimbalkar, S. & Khabbaz, H. 2020. Analytical Evaluation of Ballasted Track Substructure Response under Repeated Train Loads. *International Journal of Geomechanics*, 20, 04020093.

Sayeed, M. A. & Shahin, M. A. 2016. Three-dimensional numerical modelling of ballasted railway track foundations for high-speed trains with special reference to critical speed. *Transportation Geotechnics*, 6, 55–65.

Sheng, X., Jones, C. & Petyt, M. 1999. Ground vibration generated by a harmonic load acting on a railway track. *Journal of sound and vibration*, 225, 3–28.

Suiker, A. S., Chang, C. S., De Borst, R. & Esveld, C. 1999. Surface waves in a stratified half space with enhanced continuum properties. Part 1: Formulation of the boundary value problem. *European Journal of Mechanics-A/Solids*, 18, 749–768.

Tucho, A., Indraratna, B. & Ngo, T. 2022. Stress-deformation analysis of rail substructure under moving wheel load. *Transportation Geotechnics*, 36, 100805.

Yang, L., Powrie, W. & Priest, J. 2009. Dynamic stress analysis of a ballasted railway track bed during train passage. *Journal of Geotechnical and Geoenvironmental Engineering*, 135, 680–689.